Electronic Supplementary Material (ESI) for ChemComm.

Electronic Supporting Information

Highly dynamic metal exchange in anthrax lethal factor involves the occupation of an inhibitory metal binding site

Calvin J. Young and Stefan Siemann

Department of Chemistry and Biochemistry, Laurentian University, Sudbury, ON, P3E 2C6, Canada

Table of Contents

Experimental Procedures:

General

Chromogenic anthrax lethal factor substrate II, *S*-*p*NA (Ac-Gly-Tyr-β-Ala-Arg-Arg-Arg-Arg-Arg-Arg-Arg-Arg-Val-Leu-Arg-*p*NA; *p*NA = *para*-nitroanilide) was custom-synthesized by Biomatik Corp. (Cambridge, ON, Canada). Isotope-enriched ^{70}Zn metal (^{64}Zn < 0.02%, ^{66}Zn < 0.02%, ^{67}Zn = 0.16%, ^{68}Zn = 4.49%, and ^{70}Zn = 95.35%) was obtained from Cambridge Isotope Laboratories (Tewksbury, MA), and dissolved in trace metal grade HNO_3 prior to dilution with TraceSELECT water (Sigma-Aldrich, St. Louis, MO) to afford a stock solution of 50 mM $Zn(NO_3)_2$. All other chemicals were purchased from Sigma-Aldrich. Unless stated otherwise, all solutions were prepared with MilliQ ultrapure water (≥ 18.2 MΩ cm resistivity). To minimize contamination by trace metals, buffers were treated with Chelex-100 resin (Sigma-Aldrich).

Preparation of LF

Lethal factor containing its native zinc ion (ZnLF) was isolated and purified by chromatography on Q-Sepharose as described in the literature.[1] Demetallated LF (apoLF) was prepared by treatment of ZnLF with ethylenediaminetetraacetic acid (EDTA) and dipicolinic acid (DPA) as documented previously.[2] Cobalt-substituted LF (CoLF) was obtained using either the direct exchange method[1] or by reconstitution of apoLF with $CoCl_2$ according to the protocols outlined previously.[2] Copper-substituted LF (CuLF) was prepared by apoLF reconstitution with $CuSO_4$ as reported in the literature.[2] The metal content of all LF preparations including ZnLF, CoLF, CuLF and apoLF was assessed spectrophotometrically using the chromogenic chelators 4-(2-pyridylazo)resorcinol (for Zn^{2+} and Co^{2+}) and Zincon (for Cu^{2+}) as described previously.[3-5] The concentration of LF was determined from an absorption spectrum recorded between 250 and 350 nm on a Cary 60 UV-Vis spectrophotometer (Agilent Technologies, Mississauga, ON), by solving the Beer-Lambert law using the recorded absorbance at 280 nm and the corresponding extinction coefficient of $\varepsilon = 74200\ M^{-1}\ cm^{-1}$.[5]

LF activity assays

In a typical assay, 50 nM LF was supplemented with 10 μM *S*-*p*NA in 50 mM Hepes buffer (pH 7.4) at 25 °C directly prior to recording the progress of the hydrolysis reaction at 405 nm (for 60 s in 0.1 s intervals) using a Cary 60 UV-Vis spectrophotometer. Activities were determined using the slope of the trendline through the initial linear portion (5 – 10 s) of the progress curve. Although Hepes has previously been shown to weakly interact with Cu^{2+} (but not with Zn^{2+} or Co^{2+}),[6] the replacement of this buffer with non-complexing 3-(*N*-morpholino)propanesulfonic acid (MOPS; 50 mM, pH 7.4) in Cu^{2+} exchange/inhibition studies did neither lead to significant

changes in the enzymatic activity of Cu^{2+}-exchanged LF nor to alterations in the Cu^{2+}-mediated inhibition profile. This result suggests that Hepes, albeit weakly complexing, is a suitable choice of buffer for LF activity studies.

Zinc-to-copper exchange measured by stopped-flow spectrophotometry and determination of exchange progress

The zinc-to-copper exchange was monitored by stopped-flow UV-Vis spectrophotometry on an OLIS RSM-1000 spectrophotometer (OLIS Inc., Bogart, GA) using a two-syringe setup. One syringe was filled with ZnLF in Hepes buffer (50 mM, pH 7.4). The second syringe contained $CuSO_4$ and substrate (*S-p*NA) in buffer. Rapid mixing of these solutions resulted in final concentrations of 200 nM, 10 μM and 10 μM for ZnLF, $CuSO_4$ and *S-p*NA, respectively. It is important to note that the final concentration of Cu^{2+} utilized (i.e., 10 μM) has been shown previously to be non-inhibitory.[2] UV-Vis spectra were recorded for 60 s with a rate of 63 scans/s immediately following mixing. Two control samples were also prepared and measured. One control sample contained 200 nM ZnLF and 10 μM *S-p*NA (with water in place of the $CuSO_4$). The second control sample contained 200 nM CuLF and 10 μM *S-p*NA. The two control samples were used to obtain the minimal (ZnLF; indicative of 0% exchange) and maximal (CuLF; indicative of 100% exchange) progress curves for a zinc-to-copper exchange.

The decline in activity (slopes) over time observed for all three samples (shown in Fig. 1B), which can be attributed to rapid substrate depletion, was found to obscure the increase of activity expected during the zinc-to-copper exchange. To assess the degree of metal exchange and its contribution to the rate of substrate hydrolysis, the enzymatic activity of the zinc-to-copper exchange sample was calculated at three different time points (5 s, 10 s, 12 s) by determining the slope of the progress curve at the specified time using a ± 1.5 s window (e.g., the enzymatic activity after 10 s was obtained from the slope of the trend line considering all data points between 8.5 s and 11.5 s). The activities for the three time points were then compared to those of the CuLF and ZnLF control samples at the same level of substrate depletion, thus ensuring that the decrease in activity due to substrate depletion is taken into account. For instance, the enzymatic activity for the zinc-to-copper exchange sample after 5 s was compared to that at 3.4 s for the CuLF control and at 8.4 s for the ZnLF control, where an equal degree of substrate depletion was observed (i.e., at an Abs_{405} value of ~0.05; see black trend lines in Fig. 1B). The exchange progress (shown in Table S1) was then estimated for each time point using equation 1:

$$Exchange\ progress\ (\%) = \frac{(Ex_{sam} - Zn_{ctrl})}{(Cu_{ctrl} - Zn_{ctrl})} \times 100\% \qquad \text{(eq. 1)}$$

where Ex_{sam} is the enzymatic activity of the exchange sample at a specified time, and Zn_{ctrl} and Cu_{ctrl} are the enzymatic activities at the same level of substrate depletion (as the exchange sample) for the ZnLF and CuLF controls, respectively. For instance, at the 10 s time point, the

exchange progress was calculated as follows: ((0.75 – 0.35)/(1.40 – 0.35))(100%) = 38% (see Table S1).

Analysis of isotope exchange by ICP-MS and the *ttr* formalism

The (naturally abundant) zinc-to-^{70}Zn exchange was performed by incubating 7 μM ZnLF with 70 μM $^{70}Zn^{2+}$ in ammonium acetate (25 mM, pH 7.0) for the desired amount of time (ranging from 5 s to 5 min). Ammonium acetate was utilized in these experiments in lieu of Hepes buffer to avoid sulfur-based polyatomic interferences (e.g., $^{32}S^{16}O_2^+$, $^{32}S^+$ for ^{64}Zn) in the ICP-MS measurements.[7] The procedure for the 10 s exchange was repeated with either a reduced amount of $^{70}Zn^{2+}$ (7 μM) or with the addition of 150 μM Tb^{3+}. After incubation, exchange reactions were quenched by the addition of 80 μM EDTA (300 μM in the case of Tb^{3+}-supplemented samples). Samples were then immediately applied to a 2 mL Zeba spin desalting column (Thermo Fisher Scientific, Nepean, ON) previously equilibrated with ammonium acetate (25 mM, pH 7.0) according to the manufacturer's instructions (to remove extraneous, EDTA-bound metal). Following sample recovery, protein concentrations were determined as outlined above, and samples were diluted to a final volume of 2 mL using ammonium acetate (25 mM, pH 7.0).

Standards were prepared to allow for the approximation of metal concentrations in ammonium acetate (25 mM, pH 7.0). $^{70}Zn^{2+}$ and terbium standards were prepared at final concentrations of 1 ppb, 10 ppb, and 30 ppb using the 50 mM $^{70}Zn^{2+}$ stock solution and a 100 mM $TbCl_3$ solution, respectively. Zinc (naturally abundant) standards were prepared at concentrations of 1 ppb, 10 ppb, 30 ppb, 50 ppb, and 100 ppb using an ICP-MS zinc standard solution (1000 ppm in 1% [w/v] HNO_3). All solutions (both samples and standards) were supplemented with 5 ppb indium (from an ICP-MS indium standard solution; 1000 ppm in 1% [w/v] HNO_3) and 1% (w/v) trace metal grade HNO_3. Isotope counts were determined using an iCAP Q ICP-mass spectrometer (Thermo Fisher Scientific).

Following the measurement of metal isotopes (^{64}Zn, ^{66}Zn, ^{67}Zn, ^{68}Zn, ^{70}Zn) by ICP-MS, the data was analyzed using a tracer-to-tracee ratio (*ttr*) formalism[8-13] which allows for the determination of the number of metal ions exchanged in a system when the tracer (metal introduced into the system) and tracee (metal originally present in the system) have different isotopic distributions. The $ttr^{(x,y)}$ value can be calculated for any system with known isotopic distributions for both tracer and tracee, and the experimentally determined (by ICP-MS) isotope ratio ($r^{(x/y)}$) of the enriched isotope, *x*, and a reference isotope, *y*, using equation 2:

$$ttr^{(x,y)} = \frac{r^{(x/y)} - r^{(x)}_{tracee}}{r^{(x)}_{tracer} - r^{(x/y)}} \left(\sum_{i=1}^{z} r^{(i)}_{tracer} \Big/ \sum_{i=1}^{z} r^{(i)}_{tracee} \right) \qquad \text{(eq. 2)}$$

where $r^{(i)}$ is the isotope ratio of nuclide *i* and reference isotope *y*, $r^{(x)}$ denotes the quotient of abundances of isotopes *x* and *y* of either the tracer or tracee, and *z* denotes the number of stable isotopes (*z* = 5 for zinc).

In the case of the (naturally abundant) zinc-to-^{70}Zn exchange, the $ttr^{(x,y)}$ value was obtained using the experimentally determined $r^{(70/64)}$ ratios, with ^{64}Zn serving as the reference isotope. Based on the values presented in Table S2, equation 2 can be rewritten in the following form:

$$ttr^{(70,64)} = \frac{r^{(70/64)} - 0.0127}{4767.5 - r^{(70/64)}} (5002/2.0454) \qquad \text{(eq. 3)}$$

The $ttr^{(x,y)}$ value can be used to determine the number of ions exchanged in the system (*N* value) with the aid of the following equation:

$$N = n\left(\frac{ttr^{(x,y)}}{ttr^{(x,y)} + 1}\right) \qquad \text{(eq. 4)}$$

where n is the number of metal binding sites available ($n = 1$ in the case of LF). The kinetics of metal exchange in LF were assessed by recording the ^{70}Zn/^{64}Zn ratios as a function of the time of $^{70}Zn^{2+}$ exposure.

Mode of Zn^{2+} inhibition

The enzymatic activity of ZnLF (50 nM) was determined for various concentrations of substrate (*S*-*p*NA; ranging from 3 μM to 10 μM) and inhibitor (Zn^{2+}; ranging from 0 μM to 30 μM) in Hepes buffer (50 mM, pH 7.4) at room temperature to obtain information regarding the mode of inhibition. The recorded initial velocity data was fit to various inhibition modalities (competitive, uncompetitive, mixed-type, non-competitive)[14] using GraFit 4.0 data analysis software (Erithacus Ltd., Staines, UK), with the best fit being obtained using a pure non-competitive model (K_I = 28 (± 2) μM; see main text).

Calculation of fractional occupancies

The fractional occupancies of the inhibitory site expected during the two zinc-to-^{70}Zn exchange reactions (using 7 μM and 70 μM $^{70}Zn^{2+}$) were estimated using the determined inhibition constant (see above). For either of the concentrations of extraneous $^{70}Zn^{2+}$, the concentration of enzyme containing an inhibitory Zn^{2+} ion (E_{Zn_I}) can be determined using equation 6 (derived from equation 5):

$$K_I = \frac{(E_{tot} - E_{Zn_I})(Zn_{tot} - E_{Zn_I})}{E_{Zn_I}} \qquad \text{(eq. 5)}$$

$$\left(E_{Zn_I}\right)^2 - (Zn_{tot} + E_{tot} + K_I)E_{Zn_I} + (Zn_{tot}E_{tot}) = 0 \qquad \text{(eq. 6)}$$

where Zn_{tot} is the total concentration of (extraneous) zinc, E_{tot} is the total enzyme concentration, and K_I is the inhibition constant (which is identical to the dissociation constant of the inhibitory ion). Using the experimentally determined K_I value (28 μM), and the concentration of 7 μM for E_{tot}, E_{Zn_I} was determined by solving the quadratic equation (eq. 6). The fractional occupancy of the inhibitory site was then calculated using equation 7:

$$Occupancy = \frac{E_{Zn_I}}{E_{tot}} \times 100\% \qquad \text{(eq. 7)}$$

In the case of the zinc-to-^{70}Zn exchange with 7 μM $^{70}Zn^{2+}$ (Zn_{tot}), the occupancy of the inhibitory site was found to be 17%, whereas that for the exchange with 70 μM $^{70}Zn^{2+}$ was 70% (see main text).

Supplementary Tables:

Table S1. Enzymatic activities and exchange progress during the zinc-to-copper exchange measured under stopped-flow conditions.

Exchange time (s)	Enzymatic activity [$\Delta Abs_{405} \times 10^2\ s^{-1}$] [a]			Exchange progress (%) [b]
	Exchange sample	CuLF control	ZnLF control	
5	0.85	1.81	0.54	25
10	0.75	1.40	0.35	38
12	0.61	0.93	0.21	56

[a] Enzymatic activities for the exchange sample were determined using the slope of the trend line for all data points at the time specified (± 1.5 s). The enzymatic activities for the controls were calculated at time points where the level of substrate depletion was identical to that observed for the exchange sample.

[b] The exchange progress was estimated using equation 1.

Table S2. Isotope abundance of zinc and isotope ratios of tracee and enriched ^{70}Zn tracer.

	Abundance		Isotope ratio	
Isotopes	Tracee [a]	^{70}Zn tracer	Tracee	^{70}Zn tracer
64	0.4889	0.0002	1.0000	1.0
66	0.2781	0.0002	0.5688	1.0
67	0.0411	0.0016	0.0841	8.0
68	0.1857	0.0449	0.3798	224.5
70	0.0062	0.9535	0.0127	4767.5
SUM	**1.0000**	**1.0000**	**2.0454**	**5002.0**

[a] Values for the natural isotope abundance of zinc were taken from: *Handbook of Chemistry and Physics (51st Edition);Weast, R. C., Ed.; CRC Press, Cleveland, 1970-1971*.

Supplementary Figures:

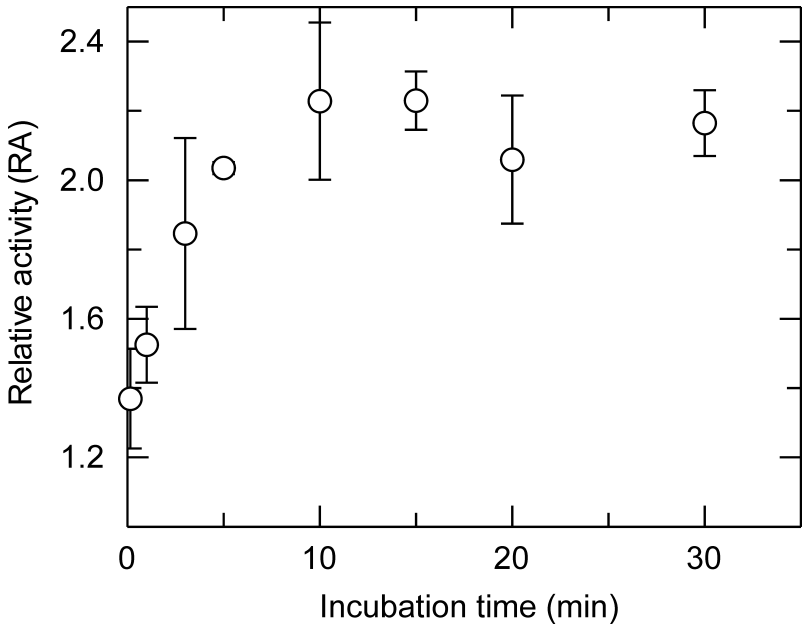

Figure S1. Time-dependence of zinc-to-cobalt exchange in LF. ZnLF (50 nM) was incubated in the presence of 1 mM Co^{2+} in Hepes buffer (50 mM, pH 7.4) at room temperature for the time indicated in the figure prior to the addition of *S*-*p*NA (10 μM) to initiate substrate hydrolysis (recorded at 405 nm). Relative activity is defined as the activity relative to that recorded in the absence of Co^{2+}. Values shown represent the mean ± 1 s.d. of three independent experiments.

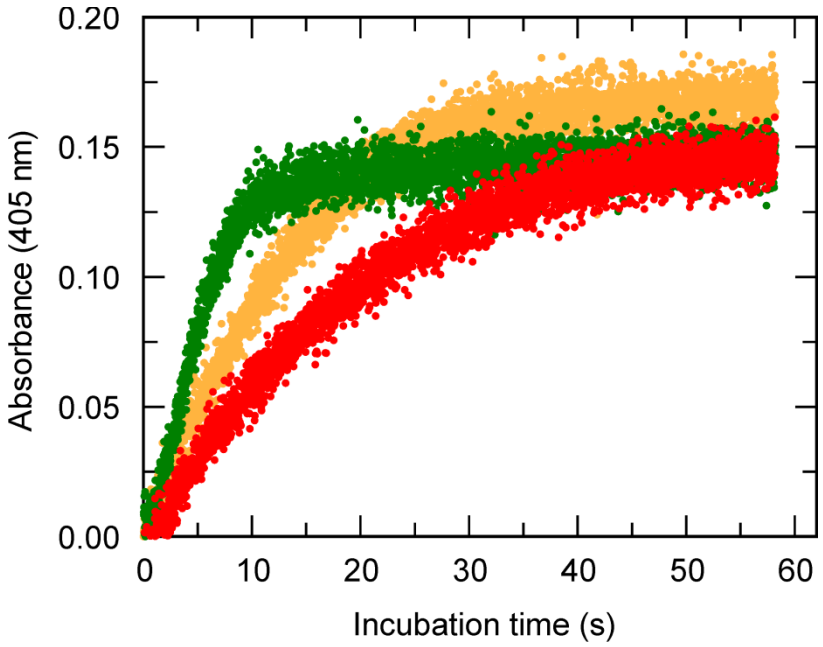

Figure S2. Full progress curves of the zinc-to-copper exchange in LF. Experiments were performed as described in the caption of Fig. 1 (panel B) in the main text. The progress curves for ZnLF, CuLF and ZnLF exposed to Cu^{2+} are shown in red, green and gold, respectively.

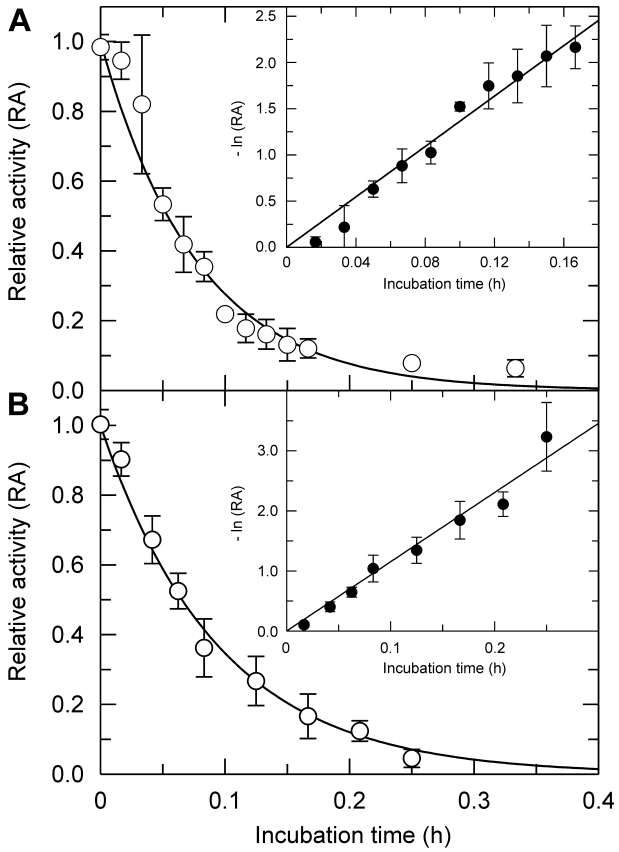

Figure S3. Effect of EDTA on the activity of CoLF (A) and CuLF (B). CoLF (50 nM) or CuLF (50 nM) were incubated in the presence of 10 mM EDTA in Hepes buffer (50 mM, pH 7.4) for the desired amount of time at room temperature prior to the addition of *S*-*p*NA (10 μM) to initiate the hydrolysis reaction. The progress of the reaction was monitored at 405 nm. Relative activity (RA) is defined as the activity relative to that recorded for CoLF or CuLF in the absence of EDTA. Values shown represent the mean ± 1 s.d. of three independent experiments. The solid line in each plot denotes the best fit of the data to the first-order rate law with k_{off} (dissociation rate constant) serving as the fitting parameter. Insets: Replot of the data showing the linear relationship between –ln (RA) and incubation time.

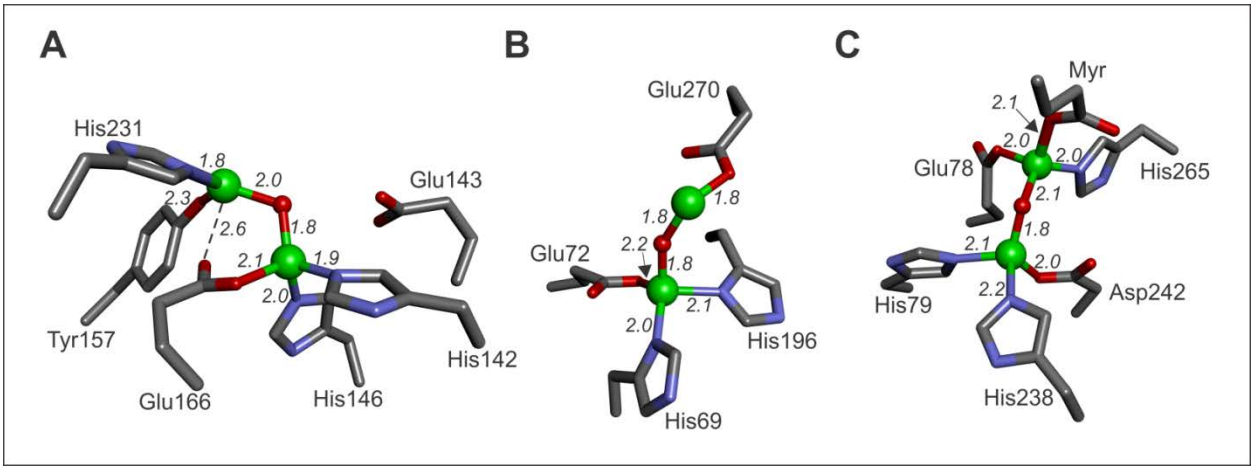

Figure S4. Structural representation of the active sites of three zinc enzymes in their zinc-inhibited forms. The structures of thermolysin (A), carboxypeptidase A (B), and LpxC (C) were generated from the PDB files 1LND,[15] 1CPX,[16] and 1P42,[17] respectively. Both the catalytic and inhibitory Zn^{2+} ions are depicted in green, with the bridging water (or hydroxide) molecule shown in red. Bond lengths are expressed in Å. Myr (panel C) denotes myristate, of which only the carboxylate-bearing part of the molecule is shown.

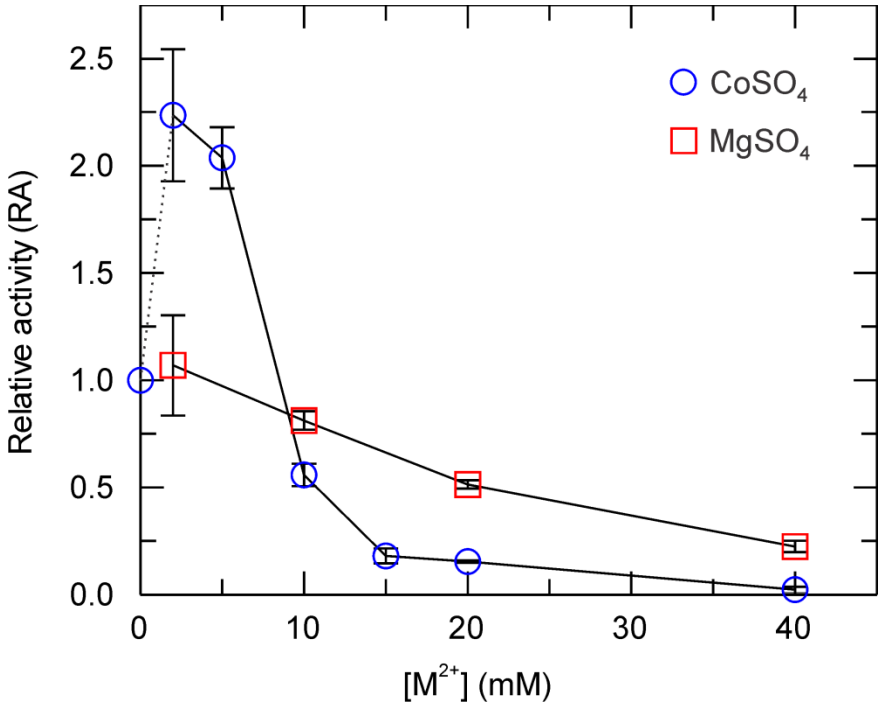

Figure S5. Effect of $CoSO_4$ (blue circles) and $MgSO_4$ (red squares) on ZnLF activity. ZnLF (50 nM) was incubated with $CoSO_4$ or $MgSO_4$ at the desired concentrations in Hepes buffer (50 mM, pH 7.4) prior to the addition of *S*-*p*NA (10 μM), and measurement of substrate hydrolysis at 405 nm. Relative activity is defined as the activity relative to that recorded in the absence of Co^{2+} or Mg^{2+}. Data points portraying to the 2.25-fold increase in activity in the sub-millimolar Co^{2+} concentration range (a consequence of zinc-to-cobalt exchange) have been omitted for the sake of clarity, and are represented by the dotted line. Values represent the mean ± 1 s.d. of three independent experiments. Since both $CoSO_4$ and $MgSO_4$ possess identical ionic strengths, the (only) slight inhibition of LF by the latter salt illustrates that the sharp decline in activity at $[Co^{2+}] > 5$ mM is not due to an ionic strength effect but rather a reflection of the inhibitory action of the transition metal ion.

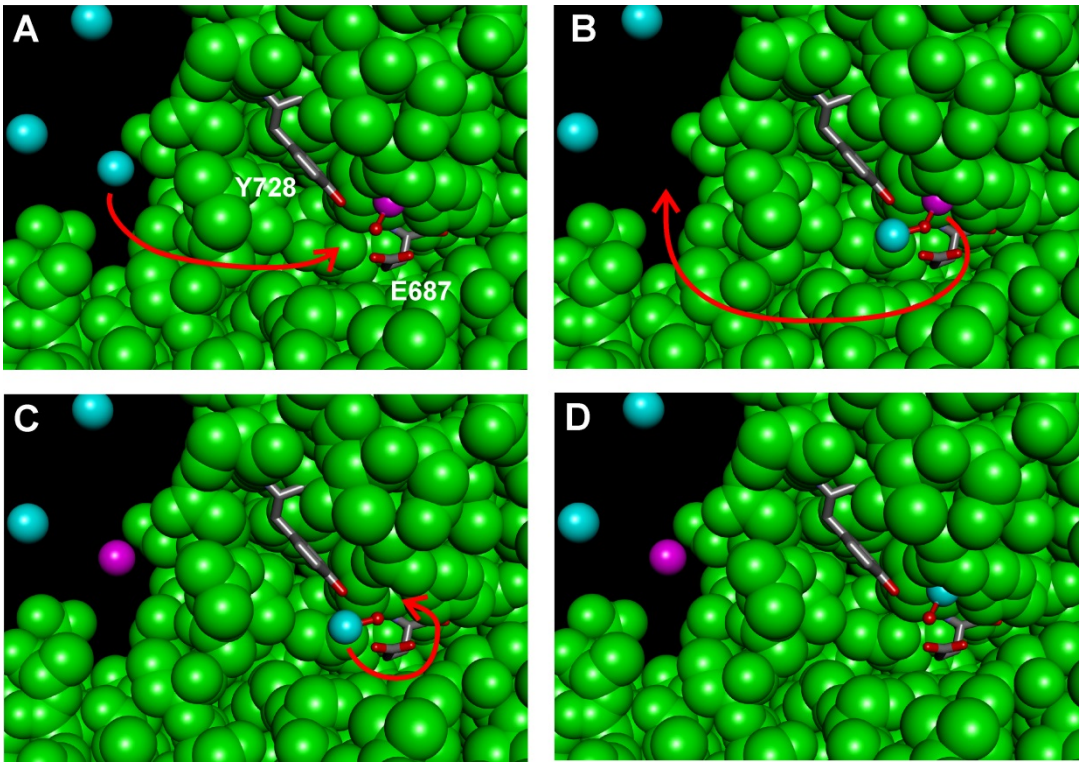

Figure S6. Proposed mechanism of metal exchange in LF. The substrate binding pocket of LF (pdb: 1J7N)[18] is shown in green, originally bound metal in magenta, and extraneous (exchanging) metal in cyan. The two residues (Tyr728 and Glu687) potentially involved in coordinating the inhibitory metal are depicted as stick models. In the proposed mechanism, the diffusion of the extraneous metal ion into the inhibitory metal binding site (A) leads to the formation of a hydroxide-bridged bimetallic species (B), in which the affinity for the active site ion is substantially decreased (e.g., through electrostatic repulsion). Following dissociation of the active site ion (C), the process of metal exchange is completed by migration of the inhibitory (and previously extraneous) metal ion into the active site (D).

References

1. C. E. Säbel, R. Carbone, J. R. Dabous, S. Y. Lo and S. Siemann, *Biochem. Biophys. Res. Commun.*, 2011, **416**, 106-110.
2. S. Y. Lo, C. E. Säbel, M. I. Webb, C. J. Walsby and S. Siemann, *J. Inorg. Biochem.*, 2014, **140**, 12-22.
3. C. E. Säbel, J. L. Shepherd and S. Siemann, *Anal. Biochem.*, 2009, **391**, 74-76.
4. C. E. Säbel, J. M. Neureuther and S. Siemann, *Anal. Biochem.*, 2010, **397**, 218-226.
5. C. E. Säbel, S. St-Denis, J. M. Neureuther, R. Carbone and S. Siemann, *Biochem. Biophys. Res. Commun.*, 2010, **403**, 209-213.
6. M. Sokołowska and W. Bal, *J. Inorg. Biochem.*, 2005, **99**, 1653-1660.
7. T. W. May and R. H. Wiedmeyer, *At. Spectrosc.*, 1998, **19**, 150-155.
8. G. Toffolo, D. M. Shames, A. Stevanato and C. Cobelli, in *Advances in Isotope Methods for the Analysis of Trace Elements in Man*, eds. N. Lowe and M. Jackson, CRC Press, Boca Raton, 2001, pp. 43-57.
9. L. R. Woodhouse and S. A. Abrams, in *Advances in Isotope Methods for the Analysis of Trace Elements in Man*, eds. N. Lowe and M. Jackson, CRC Press, Boca Raton, 2001, pp. 1-22.
10. C. Cobelli, G. Toffolo, D. M. Bier and R. Nosadini, *Am. J. Physiol.*, 1987, **253**, E551-E564.
11. C. Cobelli, G. Toffolo and D. M. Foster, *Am. J. Physiol.*, 1992, **262**, E968-E975.
12. W. T. Buckley, *Proc. Nutr. Soc.*, 1988, **47**, 407-416.
13. S. Siemann, H. R. Badiei, V. Karanassios, T. Viswanatha and G. I. Dmitrienko, *Chem. Commun.*, 2006, 532-534.
14. R. B. Silverman, *The Organic Chemistry of Enzyme-Catalyzed Reactions*, Academic Press, San Diego, 2000.
15. D. R. Holland, A. C. Hausrath, D. Juers and B. W. Matthews, *Protein Sci.*, 1995, **4**, 1955-1965.
16. J. T. Bukrinsky, M. J. Bjerrum and A. Kadziola, *Biochemistry*, 1998, **37**, 16555-16564.
17. D. A. Whittington, K. M. Rusche, H. Shin, C. A. Fierke and D. W. Christianson, *Proc. Natl. Acad. Sci. U.S.A.*, 2003, **100**, 8146-8150.
18. A. D. Pannifer, T. Y. Wong, R. Schwarzenbacher, M. Renatus, C. Petosa, J. Bienkowska, D. B. Lacy, R. J. Collier, S. Park, S. H. Leppla, P. Hanna and R. C. Liddington, *Nature*, 2001, **414**, 229-233.